


Clock generator based on a vortex attractor in polariton superfluidsXuemei Sun,¹ Gang Wang,^{1,*} Kailin Hou,¹ Huarong Bi,¹ Yan Xue^{1,†} and Alexey Kavokin^{2,3,‡}¹College of Physics, Jilin University, Changchun 130012, China²School of Science, Westlake University, 18 Shilongshan Road, Hangzhou 310024, Zhejiang Province, China³Westlake Institute for Advanced Study, Institute of Natural Sciences, 18 Shilongshan Road, Hangzhou 310024, Zhejiang Province, China (Received 28 February 2021; revised 20 January 2024; accepted 18 March 2024; published 1 April 2024)

We reveal the topologically protected persistent oscillatory dynamics of a polariton superfluid which is driven nonresonantly by a super-Gaussian laser beam in a planar semiconductor microcavity subjected to an external C-shaped potential. We find persistent oscillations characterized by an attractor of vortices that are based on the dynamical behavior of small Josephson vortices rotating around the outer boundary of the ring-shaped dense region of the central vortex. The attractor is formed due to the inverse energy cascade accompanied by the growth of incompressible kinetic energy. The attractor displays a remarkable stability towards perturbations, and it may be tuned by the pump laser intensity to two distinct frequency ranges: 20.16 ± 0.14 and 48.4 ± 1.2 GHz. This attractor is bistable with respect to the chirality of the vortex. The switching between two stable states is achieved by altering the pump power or by adding an extra incoherent Gaussian pump beam.

DOI: [10.1103/PhysRevB.109.155301](https://doi.org/10.1103/PhysRevB.109.155301)**I. INTRODUCTION**

Exciton-polariton condensates [1–3] offer intriguing possibilities for on-chip simulation of a broad variety of nonlinear phenomena in classical [4–6] and quantum [7–9] physics. The nonlinearity that is essential for these phenomena arises from the fact that the material component of exciton-polaritons allows them to interact among themselves [10,11]. On top of this, being bosonic quasiparticles, polaritons possess the remarkable ability to form superfluids even at high temperatures [12–14]. This superfluid behavior is conveniently described by a many-body wave function that is governed by a generalized Gross-Pitaevskii equation. The generalization is required to account for pumping and dissipation, which are always present in any polariton system because of the finite (and usually very short) lifetime of each individual polariton. The driven-dissipative nature of polariton superfluids is responsible for a multitude of fascinating phenomena [15–18]. To be more specific, thanks to pumping and dissipation, every polariton system is out of thermal equilibrium, and it does not strive to minimize its energy. Polariton condensates may be formed in an excited state of the lower polariton dispersion branch [19–21] or even in a superposition of excited states [22–24] of the conservative Hamiltonian of the system as long as the pumping is on.

The stationary state of a superfluid is governed by the balance of pump and decay. If the initial state of the superfluid is a superposition of two eigenstates of the Hermitian part of the Hamiltonian of the system and this state is close to the stationary state, the subsequent dynamics of the superfluid

may be characterized by the exciting phenomenon of persisting oscillations. Such oscillations manifest through periodic modulations of the density of polaritons, through the phase of the condensate, or through the spatial redistribution of either of the two. In the latter case, oscillations of quantized vortices [25,26] may be found. Quantized vortices are the subject of detailed experimental study in polaritonics. They can be conveniently identified by near-field interferometry.

A variety of physical mechanisms may be behind the formation of persistent currents or vortices in polariton superfluids. A comparison of the polariton system to the ac Josephson currents of Cooper pairs might be instructive or deceptive, depending on how the system responds to its initial conditions. If the initial state of the system is formed by a superposition of two eigenstates of the Hermitian component of the Hamiltonian, the ac Josephson current is formed [27,28]. In contrast, if the system's stationary dynamics and the initial state are mismatched, chaotic dynamics might emerge, provoking an inverse energy cascade [29,30] in which vortical structures, from small ones to large ones, form increasingly over time. The appearance of corotating pairs of vortices [31] is one of the signatures of this mechanism [32,33].

In this work, we report the persistent nonlinear dynamics of an attractor [34,35] of vortices in a circular polariton superfluid, where Josephson vortices with relatively small cores can consistently circulate around the outer boundary of the ring-shaped dense region of the central large vortex. By analyzing the dynamics of the system, we establish that the appearance of corotating pairs of vortices, induced by the inverse energy cascade triggered during the dynamical procedure of the chaotic phase of repeated collisions of vortices, is crucial to the formation of this attractor. Topological protection guarantees the robustness of the attractor dynamics, characterized by persistent oscillations over time, against external perturbations, thus preventing them from being easily disrupted.

*wg@jlu.edu.cn

†xy4610@jlu.edu.cn

‡a.kavokin@westlake.edu.cn

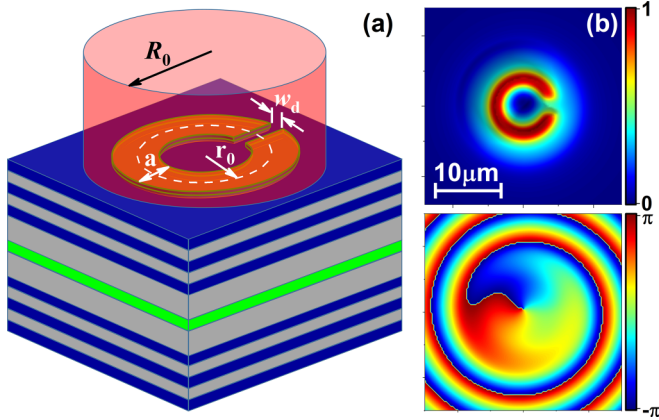


FIG. 1. (a) Sketch of the semiconductor microcavity containing a C-shaped potential, excited by a nonresonant pump in the super-Gaussian shape with radius $R_0 = 10 \mu\text{m}$. (b) Stable state of the vortex achieved with $P_0 = 3.1P_{th}$. The parameters for a C-shaped potential with a slot are $r_0 = 4 \mu\text{m}$, $a = 2 \mu\text{m}$, $w_d = 2 \mu\text{m}$, and potential depth $V_0 = -0.6 \text{ meV}$.

The system may be considered a “clock generator” [36,37] which presents remarkable stability and may be adjusted to two distinct frequency domains by tuning the pump laser intensity. Since a vortex has chiral symmetry, every attractor is bistable. In each particular numerical experiment, the system spontaneously relaxes to one of two stationary solutions. These findings provide a proof-of-concept demonstration of the feasibility of a portable and low-power clock generator based on a polariton superfluid.

II. MODEL

To be specific, we consider the system shown schematically in Fig. 1(a). The nonresonant cw optical field with the super-Gaussian shape $P(r) = P_0 e^{-(\frac{r}{R_0})^{20}}$ is applied to excite exciton-polaritons in a semiconductor microcavity containing a C-shaped in-plane external potential. r_0 and a are the radius and width of the potential ring, respectively. V_0 is the potential depth, and w_d is the width of the potential slot. Obeying the bosonic statistics, polaritons form a Bose-Einstein condensate which remains localized under the joint confinement effect of the external potential and the pump spot.

The dynamics of a polariton condensate can be described by the dissipative Gross-Pitaevskii equation for the macroscopic wave function $\psi(\mathbf{r}, t)$ coupled to the rate equation for the density of the exciton reservoir $n_R(\mathbf{r}, t)$:

$$i\hbar \frac{\partial \psi(\mathbf{r}, t)}{\partial t} = \left[-\frac{\hbar^2}{2m} \nabla^2 + g_C |\psi(\mathbf{r}, t)|^2 + g_R n_R(\mathbf{r}, t) + V(r) + \frac{i\hbar}{2} (R n_R(\mathbf{r}, t) - \gamma_C) \right] \psi(\mathbf{r}, t) + i\hbar \frac{dW}{dt},$$

$$\frac{\partial n_R(\mathbf{r}, t)}{\partial t} = P(\mathbf{r}) - [\gamma_R + R |\psi(\mathbf{r}, t)|^2] n_R(\mathbf{r}, t), \quad (1)$$

where $m = 1 \times 10^{-4} m_e$ (m_e is the free electron mass) is the effective mass of polaritons on the lower-polariton branch. The nonlinear coefficients $g_C = 3 \times 10^{-3} \text{ meV } \mu\text{m}^2$ and

$g_R = 2gc$ represent the strengths of polariton interactions among themselves and with the reservoir exciton, respectively. $\gamma_C = 0.4 \text{ ps}^{-1}$ and $\gamma_R = 0.8 \text{ ps}^{-1}$ are the polariton and reservoir decay rates, respectively. $R = 0.01 \text{ ps}^{-1} \mu\text{m}^2$ is the rate of stimulated scattering of quasiparticles from the exciton reservoir to the polariton fluid. $P(\mathbf{r})$ is the nonresonant cw optical pump. $V(\mathbf{r})$ is the external potential with depth, which can be generated in planar semiconductor microcavities using different techniques [38,39]. dW describes the quantum fluctuations within the classical field approximation with the addition of a complex stochastic term in the truncated Wigner approximation [40],

$$\langle dW(\mathbf{r}, t) dW(\mathbf{r}', t') \rangle = 0,$$

$$\langle dW(\mathbf{r}, t) dW^*(\mathbf{r}', t') \rangle = \frac{dt}{2dxdy} (R n_R + \gamma_C) \delta_{\mathbf{r}, \mathbf{r}'} \delta_{t, t'}. \quad (2)$$

III. AN ATTRACTOR OF VORTICES

The polariton superfluid, due to its non-Hermitian nature, requires a persistent external pump to sustain the polariton population by means of the stimulated scattering of quasiparticles from the exciton reservoir to the polariton reservoir. The spatial characteristics of the pump have a notable influence on the reservoir-induced effective potential confining the condensate, which, in conjunction with the external potential, plays a crucial role in determining the dynamics of the superfluid system. For instance, in the case of a polariton superfluid confined within an external C-shaped potential, although Josephson vortex pairs form at the location of the potential slot functioning as a Josephson junction, the ultimate stationary state hinges on the profiles of the pumping mechanism. If the pump exhibits an annular configuration, the superposition of two eigenstates of the Hermitian part of the Hamiltonian of the system can be excited, and the subsequent dynamics of the superfluid may be characterized by quantum beats with a characteristic frequency dependent on the energy splitting of the involved eigenstates [27]. If the pump, however, exhibits a super-Gaussian profile, only one excited state with two modes is stimulated, and the subsequent dynamics of the superfluid may manifest in the periodic oscillation where Josephson vortices with relatively small objects can consistently circulate around the outer boundary of the ring-shaped dense region of the density of the central large vortex. We shall refer to the cyclic dynamics, demonstrated by the system, as an attractor of vortices. The attractor of vortices is similar to a limit cycle attractor [34,35], in which it concerns the ability of returning to a stable periodic orbit even after being perturbed. Two types of attractors of vortices, presented in Fig. 2, emerge spontaneously due to the random fluctuations of the initial noise and the quantum fluctuation dW . Attractor A, as seen in Figs. 2(a1)–2(a3), illustrates the periodic rotation of a single small Josephson vortex around the outer edge of the annular density of the central vortex. Conversely, Figs. 2(b1)–2(b3), showing attractor B, depict the periodic rotation of two small Josephson vortices. The former is accomplished by utilizing a pump power of $P_0 = 2.9P_{th}$, while the latter is obtained by employing a slightly lower pump power of $P_0 = 2.6P_{th}$. In both scenarios, all small Josephson vortices exhibit circulation identical to

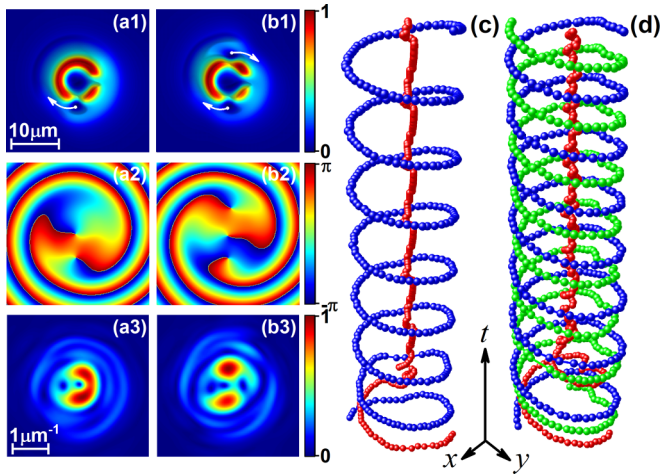


FIG. 2. Attractor of vortices. (a1) and (b1) Polariton density in real space, (a2) and (b2) phase distribution in real space, and (a3) and (b3) polariton density in momentum space for two different pump powers. (a) One small Josephson vortex ($P_0 = 2.9P_{th}$) or (b) two small Josephson vortices ($P_0 = 2.6P_{th}$) circulate around the outer edge of the annular density of the central large vortex. White arrows depict the direction of movement of the Josephson vortices. (c) and (d) The trajectories of the vortex singularity in the xyt space for the attractor of vortices in (a) and (b).

that of the central vortex, as depicted in Figs. 2(a2) and 2(b2), showing the phase distribution in real space. It is clear that the quantity of the Josephson vortices, which are captured as small objects by the central vortex, diminishes as the pump power increases. Hence, it is not surprising that a stable vortex state can be observed as the pump power is progressively raised to the value of $P_0 = 3.1P_{th}$, as seen in Fig. 1(b). This observation is consistent with the non-Hermitian nature of the polariton superfluid, wherein an increase in the pump power leads to a decrease in the energy of the state. Indeed, due to non-Hermitian terms, neither the number of particles nor the energy is conserved by the Hamiltonian. The stimulated scattering terms that favor the occupation of highly populated states start playing a more important role with the increase of the pump power, which eventually leads to a decrease of the mean energy per particle manifested in the numerical calculation. The effects revealed by this study diverge from those observed in polariton condensates subjected to annular external potentials. In the context of the earlier study [41], it is observed that vortex structures characterized by varying winding numbers (representing angular momentum) tend to exhibit stability when subjected to adjustments in the pump power. The limit cycles have been discussed and experimentally searched for in polariton fluids. Proposals for polariton time crystals [37,42,43] based on such limit cycles have been made. In this context, the originality of the present work is in the focus on vortex/antivortex oscillation dynamics that allows for a relatively easy experimental detection via interferometry and brings an interesting phenomenology of the Laguerre-Gaussian beams with oscillation orbital momenta.

It is important to highlight that in the context of the attractor of vortices, both the central vortex and the small Josephson vortices are close to the first excited state of the external potential where a stable vortex is normally located. The po-

lariton density distribution in momentum space, as seen in Figs. 2(a3) and 2(b3), illustrates the presence of small Josephson vortices within the annulus of the density of the central vortex. These small Josephson vortices split the central vortex into several portions to generate unbalanced modes in the first excited state. The binding energy between the central vortex and the small Josephson vortices may be approximated by calculating the vector difference of their singularity locations in momentum space. It is worth noting that the uncertainty of this estimation, denoted as Δk , is about $0.08 \mu\text{m}^{-1}$. We believe that this binding energy is responsible for the formation of an attractor. It makes our system return to a stable periodic orbit after being perturbed. We prove the stability of the observed dynamics by adding a Gaussian-shaped barrier to the path of the small Josephson vortex for several oscillating periods. Having added this perturbation, we observe that the small Josephson vortex would bypass the barrier's periphery while meeting the barrier and then continue to orbit along the original trace. Further, if the barrier is withdrawn after several oscillating periods, the small Josephson vortex would go back to its original trace.

Figures 2(c) and 2(d) illustrate the spatiotemporal trajectories of the vortex singularities within the studied attractor of vortices, with a temporal resolution of $\delta t = 1$ ps. The singularity of the central vortex remains intact as it moves within the core area, but the singularities of the rotating Josephson vortices follow a circular course. The orbital-like trajectory is analogous to that of the half vortex in a spinor polariton condensate [44], where a vortex characterized by a certain circular polarization coincides with a Gaussian beam that has the opposite circular polarization. Orbital-like trajectories suggest an attractive interaction between the central vortex and the rotating Josephson vortices.

In order to reveal the physical mechanism responsible for the formation of an attractor of vortices, it is essential to recall the physics of an inverse energy cascade. An inverse energy cascade is a physical phenomenon observed in two-dimensional (2D) fluid dynamics, in which, during the process of energy transfer, energy gradually transfers from small-scale vortices to large-scale vortices, as indicated by a Kolmogorov-like $-5/3$ power law in the kinetic energy spectrum [45,46]. Within the realm of atomic Bose-Einstein condensates [47,48], the clustering of vortices with the same rotational direction, along with the increase in the incompressible kinetic energy per vortex, is commonly recognized as the characteristic feature of an inverse energy cascade. For a dissipative polariton system, both theoretical [49,50] and experimental [30] studies have successfully illustrated the occurrence of vortex clustering, highlighting the tendency of the vortex gas towards highly excited configurations. In the following, we shall concentrate on the role of the inverse energy cascade in the generation of a corotating pair of vortices characterized by identical vortex numbers and kinetic energy [see Fig. 3(g)], which plays a critical role in the dynamics of an attractor of vortices.

Let us consider the scenario involving a single Josephson vortex playing the role of a small rotating object. The polariton density generated by the pump with $P_0 = 2.9P_{th}$ is sufficient to ensure the superfluid behavior of the polariton condensate, resulting in a shallow density distribution across

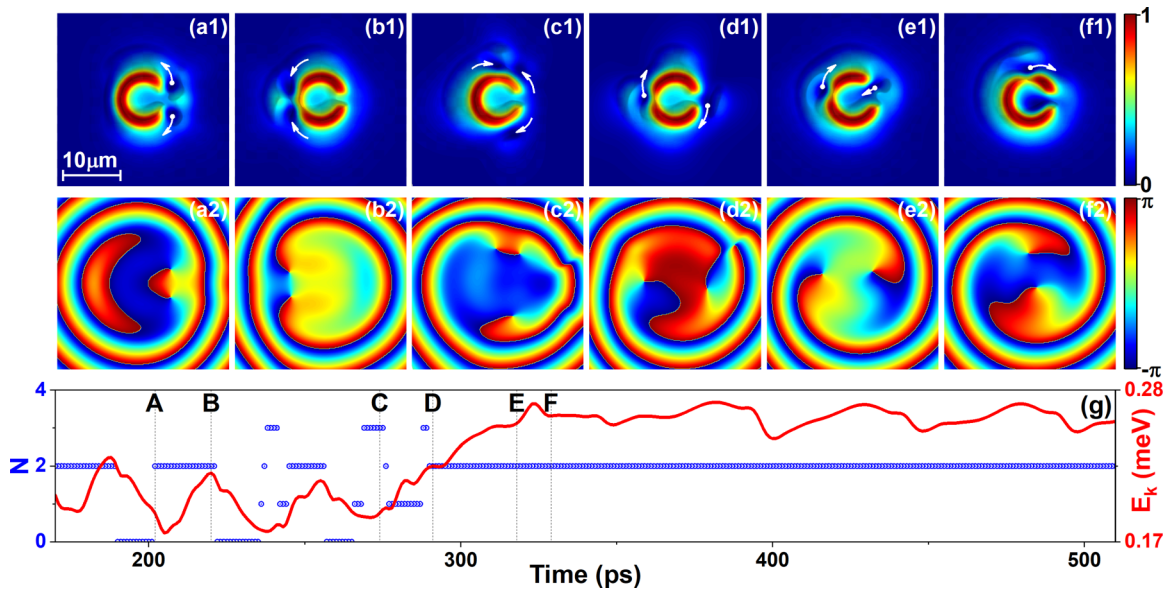


FIG. 3. (a1)–(f1) The polariton densities and (a2)–(f2) the corresponding phases in the dynamical procedure for the formation of an attractor of vortices with a single Josephson vortex orbiting around the central vortex. (g) The vortex counts and kinetic energy vs time. The inverse energy cascade is primarily responsible for the formation of an attractor.

the potential slot. This distribution disrupts the rotational symmetry of the polariton density and exhibits features similar to those of a Josephson junction. Consequently, Josephson vortex-antivortex pairs are induced symmetrically with respect to the y axis on the right side of the potential slot [see Fig. 3(a)]. The vortex and antivortex exhibit opposite rotational orientations around the outside border of the ring-shaped dense part of the polariton condensate and intersect at a specific spot symmetric to the potential slot with respect to the x axis [see Fig. 3(b)]. Following the collision, the vortex and antivortex tunnel through the dense part of the ring and subsequently undergo annihilation. Although the observed dynamical activity exhibits periodicity throughout several cycles, it does not represent a stationary state of the system. At a certain moment, this behavior is abruptly interrupted, resulting in the cessation of tunneling following the collision. One vortex loses its energy following the impact and progressively diminishes over time, while the other vortex persists in its rotational motion at the outer boundary of the ring-shaped dense part of the polariton condensate [see Fig. 3(c)]. Therefore, the left vortex is inevitably hit with the newly generated vortex or antivortex. In a 2D condensate, the occurrence of repeated collisions between vortices can give rise to an inverse energy cascade, which is facilitated by the inclusion of the quantum pressure term $|\psi|^2 \nabla \cdot \left(\frac{\hbar^2 \nabla^2 |\psi|}{2m |\psi|} \right)$ [51] in the Gross-Pitaevskii equation. As a result of this inverse energy cascade, vortex reconnection takes place, leading to the annihilation of vortices possessing a particular circulation and the generation of a corotating vortex pair with the same circulation. This phenomenon is shown in Fig. 3(d): the right-circulation vortex is eliminated following the collision, whereas a corotating pair of vortices with left circulation is retained.

Figure 3(g) illustrates the fluctuations in vortex counts and the associated time dependence of the incompressible kinetic energy. The temporal intervals represented by points A to F

correspond to those in Figs. 3(a) to 3(f), respectively. It is evident that prior to the formation of the dynamics shown by C, the annihilation of the vortex through tunneling consistently coincides with a reduction in the kinetic energy. On the other hand, it is observed that the kinetic energy between points C and D steadily grows, despite the decrease in the number of vortices resulting from collisions. The occurrence of a corotating pair of vortices provides direct proof of the inverse energy cascade.

The sequence of events following the formation of a corotating vortex pair is straightforward to interpret. Governed by the Magnus force $F_M = 2\pi \hbar m |\psi|^2 \vec{e}_z \times \vec{v}_{\text{rel}}$ [52], the corotating vortex pair keeps orbiting the outer boundary of the ring-shaped dense region of the condensate until one vortex meets the potential slot. The attenuated polariton density within this slot modulates the effective Magnus force, consequently drawing the small Josephson vortex into the core of the ring-shaped condensate [see Fig. 3(e)]. This inward spiral leads to the excitation of a central vortex, yet it does not affect the trajectory of the remaining vortices, which persist as compact entities that continuously rotate around the central vortex [see Fig. 3(f)]. Altogether, this produces a dynamically stable vortex attractor. Once the direction of the oscillation is established, it remains unaltered.

The periodic rotation of Josephson vortices around the central vortex makes the attractor of vortices behave like a clock generator. A key figure of merit for clocks is the achievable oscillation frequency and stability. To illustrate these characteristics, we plot in Figs. 4(a) and 4(b) the temporal dependences of the polariton density at the fixed point ($x = -5, y = 0$) for attractors A and B, respectively, corresponding to Figs. 2(a) and 2(b). The center of the moving Josephson vortices passes through the considered point from time to time. High-contrast stable periodic oscillations are visible. These oscillations begin at around 100 ps and

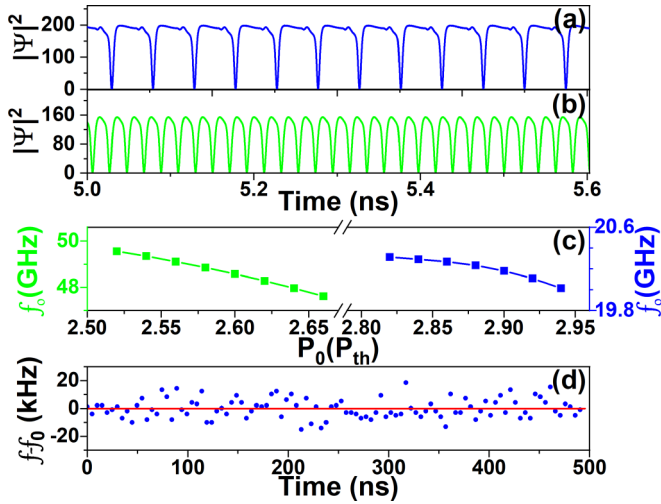


FIG. 4. The frequency of oscillations exhibited by the attractor of vortices. (a) and (b) The time dependences of the polariton density at the fixed point ($x = -5$, $y = 0$), corresponding to Figs. 2(a) and 2(b), respectively. (c) The dependence of the frequency of oscillations on the pump power. (d) The time-resolved numerical measurement of the oscillation frequency offset from the mean ~ 20.18 GHz output frequency.

remain stable for at least 500 ns, with no sign of decay or dephasing. We checked that the period of oscillations over this time range remains perfectly stable even though the static potential noise is taken into account in the calculation. Figure 4(c) predicts the dependence of the oscillation frequency on the pump power, a parameter that can be tuned easily in the experiments. Two frequency ranges around 20.16 ± 0.14 and 48.4 ± 1.2 GHz are visible. The higher the pump power is, the lower the oscillation frequency is. We believe that modulating the pump power is the easiest way to tune the operation frequency, although other parameters affecting the external potential can also be modulated. It is important to note that the impact of the up to 5% intensity fluctuation of the pump laser on the oscillation frequency is negligible, as our calculations show. Figure 4(d) presents the time-resolved numerical measurement of the 20.18 GHz clock generator output over 500 ns, which corresponds to 10 000 periods of oscillations shown in Fig. 4(a). Here, each point is the result of averaging over 100 numerical measurements with an observation time of 100 periods of oscillations. The noise is taken into account according to Eq. (2). The mean value depicted by the red solid line is in agreement with the simulation results obtained by neglecting the noise. The absolute frequency shift of our clock generator is around $\Delta f \sim 20$ kHz, and the corresponding fractional frequency stability is $\Delta f/f_0 \sim 10^{-6}$. Two-dimensional numerical simulations become too expensive if carried over a much longer time. This prevents us from predicting here the value of the Allan deviation of the stabilized clock signal to estimate the ultimate stability of the chip-scale polariton clock generator. We believe that an experimental measurement of the Allan deviation is more important than any theoretical prediction.

We also note that the polariton system is bistable due to its strong nonlinearity, which is why it relaxes to either clock-

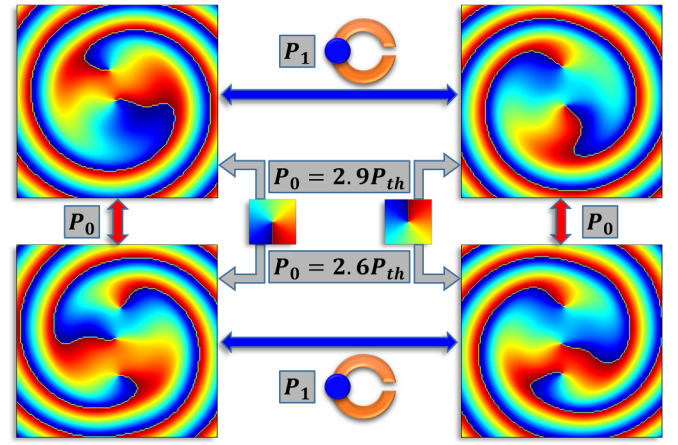


FIG. 5. The dynamical switching from any controllable state of the attractor of vortices to a desired state. The phase profiles of the target attractor of vortices are shown in the larger panels. The switch between states with the same direction of rotation is achieved by simply modulating the power of the incoherent super-Gaussian pump field P_0 . The switch between bistable states with counterrotating directions is achieved with an additional incoherent pump $P'(r)$ carrying the same direction of rotation as the target state. Phase profiles of $P'(r)$ and initial seeds are shown in the smaller panels.

wise or counterclockwise rotation stochastically, with each orientation appearing with a 50% probability. The rotation direction of a given attractor of vortices may be imprinted by seeding an initial orbital angular momentum, which is similar to the method to control the chirality of stable vortices. Figure 5 shows four examples of spontaneously formed attractor of vortices with target rotation directions defined by seeding an initial orbital angular momentum, which is depicted by two small color panels. Further, the attractor of vortices can be switched to a new one characterized by a different frequency by simply modulating the pump power P_0 (see red arrows). Additionally, it is important to note that the bistable attractor of vortices with opposite rotation directions can also be controlled by switching an additional incoherent super-Gaussian pump $P'(r) = P_1 e^{-[(x+4)^2 + y^2]/41^{10}}$ at the position symmetric to the potential slot with respect to the x axis (see blue arrows). In general, we are able to switch from any state of an attractor of vortices to any desired target state. The dynamical switch with the modulation of $P'(r)$ is shown in the movie in the Supplemental Material [53].

Through large numerical simulations, we obtain phase diagrams to observe two kinds of attractors of vortices for two considered potential depths: V_0 of either -0.6 or -0.5 meV, as shown in Fig. 6. To obtain these phase diagrams, the dynamics of the system is studied by scanning the pump power P_0 while keeping a fixed potential slot w_d . For a fixed P_0 , the attractor of vortices forms while w_d is small enough. In particular, the range of w_d where one can observe attractor of vortices A, characterized by a single Josephson vortex playing the role of a small rotating object, is larger than that for attractor of vortices B, characterized by two Josephson vortices playing the role of small rotating objects. Comparing two different ranges of pump power needed to observe the attractors of vortices for two different values of the potential

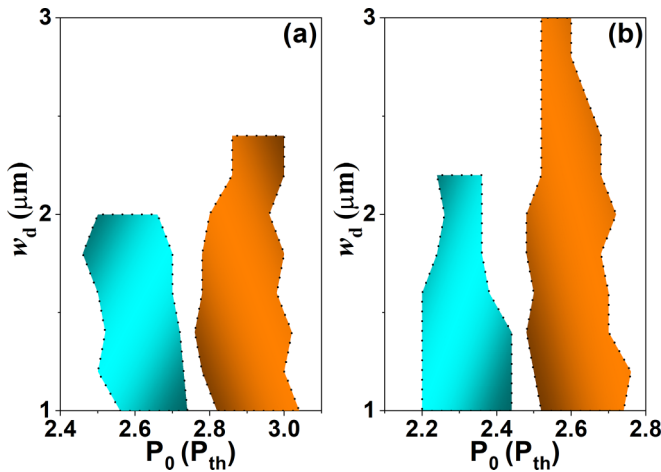


FIG. 6. The phase diagram of the existence of the attractor of vortices shown in Fig. 2 for two different potential depth: (a) $V_0 = -0.6$ and (b) -0.5 meV. The orange plot for attractor A is shown in Fig. 2(a), and the cyan plot for attractor B in shown in Fig. 2(b).

depth V_0 , one can conclude that the shallower the potential depth is, the lower the required pump power is.

IV. CONCLUSION

We predicted here the formation of the attractor of vortices in a superfluid of exciton-polaritons placed in an external lateral potential of the C-shaped geometry. The attractor of vortices corresponds to the regime where Josephson vortices are rotating periodically around a central large vortex. The inverse energy cascade was shown to be responsible for the formation of the attractor of vortices. The high stability of the oscillations makes it possible to use an attractor of vortices as a portable clock generator operating in a low-power regime. We showed that the operation frequency of the clock generator can be controlled within two different ranges. It can be tuned by tuning the laser pump power.

ACKNOWLEDGMENTS

This work was supported by the National Natural Science Foundation of China (Grant No. 12074147). A.K. acknowledges the support from Westlake University, Project No. 041020100118 and Program No. 2018R01002, funded by the Leading Innovative and Entrepreneur Team Introduction Program of Zhejiang Province.

- [1] J. Kasprzak, M. Richard, S. Kundermann, A. Baas, P. Jeambrun, J. M. J. Keeling, F. M. Marchetti, M. H. Szymańska, R. André, J. L. Staehli, V. Savona, P. B. Littlewood, B. Deveaud, and L. S. Dang, Bose-Einstein condensation of exciton polaritons, *Nature (London)* **443**, 409 (2006).
- [2] A. Amo, J. Lefrère, S. Pigeon, C. Adrados, C. Ciuti, I. Carusotto, R. Houdré, E. Giacobino, and A. Bramati, Superfluidity of polaritons in semiconductor microcavities, *Nat. Phys.* **5**, 805 (2009).
- [3] H. Deng, H. Haug, and Y. Yamamoto, Exciton-polariton Bose-Einstein condensation, *Rev. Mod. Phys.* **82**, 1489 (2010).
- [4] I. A. Shelykh, G. Pavlovic, D. D. Solnyshkov, and G. Malpuech, Proposal for a mesoscopic optical Berry-phase interferometer, *Phys. Rev. Lett.* **102**, 046407 (2009).
- [5] A. V. Zasedatelev, A. V. Baranikov, D. Urbonas, F. Scafirimuto, U. Scherf, T. Stöferle, R. F. Mahrt, and P. G. Lagoudakis, A room-temperature organic polariton transistor, *Nat. Photon.* **13**, 378 (2019).
- [6] N. G. Berloff, M. Silva, K. Kalinin, A. Askitopoulos, J. D. Topfer, P. Cilibrizzi, W. Langbein, and P. G. Lagoudakis, Realizing the classical XY Hamiltonian in polariton simulators, *Nat. Mater.* **16**, 1120 (2017).
- [7] M. Bamba, S. Pigeon, and C. Ciuti, Quantum squeezing generation versus photon localization in a disordered planar microcavity, *Phys. Rev. Lett.* **104**, 213604 (2010).
- [8] A. Delteil, T. Fink, A. Schade, S. Höfling, C. Schneider, and A. Mamolu, Emergence of quantum correlations from interacting fibre-cavity polaritons, *Nat. Mater.* **18**, 219 (2019).
- [9] S. Ghosh, K. Nakajima, T. Krisnanda, K. Fujii, and T. C. H. Liew, Quantum neuromorphic computing with reservoir computing networks, *Adv. Quantum Technol.* **4**, 2100053 (2021).
- [10] I. Carusotto and C. Ciuti, Quantum fluids of light, *Rev. Mod. Phys.* **85**, 299 (2013).
- [11] P. St-Jean, V. Goblot, E. Galopin, A. Lemaître, T. Ozawa, L. L. Gratiet, I. Sagnes, J. Bloch, and A. Amo, Lasing in topological edge states of a one-dimensional lattice, *Nat. Photon.* **11**, 651 (2017).
- [12] A. Dreismann, P. Cristofolini, R. Balili, G. Christmann, F. Pinsker, N. G. Berloff, Z. Hatzopoulos, P. G. Savvidis, and J. J. Baumberg, Coupled counterrotating polariton condensates in optically defined annular potentials, *Proc. Natl. Acad. Sci. USA* **111**, 8770 (2014).
- [13] S. Kéna-Cohen and S. R. Forrest, Room-temperature polariton lasing in an organic single-crystal microcavity, *Nat. Photon.* **4**, 371 (2010).
- [14] R. Su, J. Wang, J. Zhao, J. Xing, W. Zhao, C. Diederichs, T. C. H. Liew, and Q. Xiong, Room temperature long-range coherent exciton polariton condensate flow in lead halide perovskites, *Sci. Adv.* **4**, eaau0244 (2018).
- [15] H. Suchomel, S. Klemmt, T. H. Harder, M. Klaas, O. A. Egorov, K. Winkler, M. Emmerling, R. Thomale, S. Höfling, and C. Schneider, Platform for electrically pumped polariton simulators and topological lasers, *Phys. Rev. Lett.* **121**, 257402 (2018).
- [16] A. Dikopoltsev, T. H. Harder, E. Lustig, O. A. Egorov, J. Beierlein, A. Wolf, Y. Lumer, M. Emmerling, C. Schneider, S. Höfling, M. Segev, and S. Klemmt, Topological insulator vertical-cavity laser array, *Science* **373**, 1514 (2021).
- [17] I. Amelio, and I. Carusotto, Theory of the coherence of topological lasers, *Phys. Rev. X* **10**, 041060 (2020).
- [18] C. Huang, C. Zhang, S. Xiao, Y. Wang, Y. Fan, Y. Liu, N. Zhang, G. Qu, H. Ji, J. Han, L. Ge, Y. Kivshar, and Q. Song, Ultrafast control of vortex microlasers, *Science* **367**, 1018 (2020).
- [19] A. Muñoz Mateo, Y. G. Rubo, and L. A. Toikka, Long Josephson junctions with exciton-polariton condensates, *Phys. Rev. B* **101**, 184509 (2020).

- [20] V. N. Gladilin and M. Wouters, Noise-induced transition from superfluid to vortex state in two-dimensional nonequilibrium polariton condensates, *Phys. Rev. B* **100**, 214506 (2019).
- [21] V. Lukoshkin, E. Sedov, V. Kalevich, Z. Hatzopoulos, P. G. Savvidis, and A. Kavokin, Steady state oscillations of circular currents in concentric polariton condensates, *Sci. Rep.* **13**, 4607 (2023).
- [22] J. D. Töpfer, H. Sigurdsson, S. Alyatkin, and P. G. Lagoudakis, Lotka-Volterra population dynamics in coherent and tunable oscillators of trapped polariton condensates, *Phys. Rev. B* **102**, 195428 (2020).
- [23] S. S. Demirchyan, I. Yu. Chestnov, A. P. Alodjants, M. M. Glazov, and A. V. Kavokin, Qubits based on polariton Rabi oscillators, *Phys. Rev. Lett.* **112**, 196403 (2014).
- [24] F. I. Moxley, J. P. Dowling, W. Dai, and T. Byrnes, Sagnac interferometry with coherent vortex superposition states in exciton-polariton condensates, *Phys. Rev. A* **93**, 053603 (2016).
- [25] G. Roumpos, M. D. Fraser, A. Löffler, S. Höfling, A. Forchel, and Y. Yamamoto, Single vortex-antivortex pair in an exciton-polariton, *Nat. Phys.* **7**, 129 (2011).
- [26] T. Gao, O. A. Egorov, E. Estrecho, K. Winkler, M. Kamp, C. Schneider, S. Höfling, A. G. Truscott, and E. A. Ostrovskaya, Controlled ordering of topological charges in an exciton-polariton chain, *Phys. Rev. Lett.* **121**, 225302 (2018).
- [27] Y. Xue, I. Chestnov, E. Sedov, E. Kiktenko, A. K. Fedorov, S. Schumacher, X. Ma, and A. Kavokin, Split-ring polariton condensates as macroscopic two-level quantum systems, *Phys. Rev. Res.* **3**, 013099 (2021).
- [28] J. Barrat, A. F. Tzortzakakis, M. Niu, X. Zhou, G. G. Paschos, D. Petrosyan, and P. G. Savvidis, Qubit analog with polariton superfluid in an annular trap, [arXiv:2308.05555](https://arxiv.org/abs/2308.05555).
- [29] G. Boffetta and R. E. Ecke, Two-dimensional turbulence, *Annu. Rev. Fluid Mech.* **44**, 427 (2012).
- [30] R. Panico, P. Comaron, M. Matuszewski, A. S. Lanotte, D. Trypogeorgos, G. Gigli, M. De Giorgi, V. Ardizzone, D. Sanvitto, and D. Ballarini, Onset of vortex clustering and inverse energy cascade in dissipative quantum fluids, *Nat. Photon.* **17**, 451 (2023).
- [31] C. García and S. V. Haziot, Global bifurcation for corotating and counter-rotating vortex pairs, *Commun. Math. Phys.* **402**, 1167 (2023).
- [32] S. Kida and M. Takaoka, Vortex reconnection, *Annu. Rev. Fluid Mech.* **26**, 169 (1994).
- [33] Y. Minowa, S. Aoyagi, S. Inui, T. Nakagawa, G. Asaka, M. Tsubota, and M. Ashida, Visualization of quantized vortex reconnection enabled by laser ablation, *Sci. Adv.* **8**, eabn1143 (2022).
- [34] D. Dutta and J. K. Bhattacharjee, *Limit Cycle Oscillations, Springer Proceedings in Physics Vol. 126* (Springer, Dordrecht, 2008), p. 125.
- [35] J. Guckenheimer and P. Holmes, *Nonlinear Oscillations, Dynamical Systems, and Bifurcations of Vector Fields* (Springer, New York, 1983), pp. 66–156.
- [36] C. Leblanc, G. Malpuech, and D. D. Solnyshkov, High-frequency exciton-polariton clock generator, *Phys. Rev. B* **101**, 115418 (2020).
- [37] I. Carraro Haddad, D. L. Chafatinos, A. S. Kuznetsov, I. A. Papuccio-Fernández, A. A. Reynoso, A. E. Bruchhausen, K. Biermann, P. V. Santos, G. Usaj, and A. Fainstein, Solid-state continuous time crystal with a built-in clock, [arXiv:2401.06246](https://arxiv.org/abs/2401.06246).
- [38] R. Balili, V. Hartwell, D. Snoke, L. Pfeiffer, and K. West, Bose-Einstein condensation of microcavity polaritons in a trap, *Science* **316**, 1007 (2007).
- [39] C. W. Lai, N. Y. Kim, S. Utsunomiya, G. Roumpos, H. Deng, M. D. Fraser, T. Byrnes, P. Recher, N. Kumada, T. Fujisawa, and Y. Yamamoto, Coherent zero-state and π -state in an exciton-polariton condensate array, *Nature (London)* **450**, 529 (2007).
- [40] M. Wouters and V. Savona, Stochastic classical field model for polariton condensates, *Phys. Rev. B* **79**, 165302 (2009).
- [41] F. Barkhausen, S. Schumacher, and X. Ma, Multistable circular currents of polariton condensates trapped in ring potentials, *Opt. Lett.* **45**, 1192 (2020).
- [42] G. P. Martins, O. L. Berman, and G. Gumbs, Polaritonic and excitonic time crystals based on TMDC strips in an external periodic potential, *Sci. Rep.* **13**, 19707 (2023).
- [43] A. V. Nalitov, H. Sigurdsson, S. Morina, Y. S. Krivosenko, I. V. Iorsh, Y. G. Rubo, A. V. Kavokin, and I. A. Shelykh, Optically trapped polariton condensates as semiclassical time crystals, *Phys. Rev. A* **99**, 033830 (2019).
- [44] L. Dominici, G. Dagvadorj, J. M. Fellows, D. Ballarini, M. De Giorgi, F. M. Marchetti, B. Piccirillo, L. Marrucci, A. Bramati, G. Gigli, M. H. Szymańska, and D. Sanvitto, Vortex and half-vortex dynamics in a nonlinear spinor quantum fluid, *Sci. Adv.* **1**, e1500807 (2015).
- [45] R. H. Kraichnan, Inertial ranges in two-dimensional turbulence, *Phys. Fluids* **10**, 1417 (1967).
- [46] L. Onsager, Statistical hydrodynamics, *Nuovo Cimento* **6**(Suppl. 2), 279 (1949).
- [47] S. P. Johnstone, A. J. Groszek, P. T. Starkey, C. J. Billington, T. P. Simula, and K. Helmerson, Evolution of large-scale flow from turbulence in a two-dimensional superfluid, *Science* **364**, 1267 (2019).
- [48] G. Gauthier, M. T. Reeves, X. Yu, A. S. Bradley, M. A. Baker, T. A. Bell, H. Rubinsztein-Dunlop, M. J. Davis, and T. W. Neely, Giant vortex clusters in a two-dimensional quantum fluid, *Science* **364**, 1264 (2019).
- [49] S. V. Koniakhin, O. Bleu, G. Malpuech, D. D. Solnyshkov, 2D quantum turbulence in a polariton quantum fluid, *Chaos Solitons Fractals* **132**, 109574 (2020).
- [50] N. G. Berlof, Turbulence in exciton-polariton condensates, [arXiv:1010.5225](https://arxiv.org/abs/1010.5225).
- [51] C. F. Barenghi and N. G. Parker, *A Primer on Quantum Fluids* (Springer, Berlin, 2016).
- [52] E. B. Sonin, Magnus force in superfluids and superconductors, *Phys. Rev. B* **55**, 485 (1997).
- [53] See Supplemental Material at <http://link.aps.org/supplemental/10.1103/PhysRevB.109.155301> for the dynamic switching between the two bistable states of vortex attractors A (switch-p1-a) and B (switch-p1-b), achieved with an additional incoherent pump.